

Control of the ferroelectricity in a metastable state for orthorhombic $RMnO_3$ crystals

This article has been downloaded from IOPscience. Please scroll down to see the full text article.

2007 J. Phys.: Condens. Matter 19 145279

(<http://iopscience.iop.org/0953-8984/19/14/145279>)

View [the table of contents for this issue](#), or go to the [journal homepage](#) for more

Download details:

IP Address: 129.252.86.83

The article was downloaded on 28/05/2010 at 17:37

Please note that [terms and conditions apply](#).

Control of the ferroelectricity in a metastable state for orthorhombic $RMnO_3$ crystals

K Noda, M Akaki, F Nakamura, D Akahoshi and H Kuwahara

Department of Physics, Sophia University Chiyoda-ku, Tokyo 102-8554, Japan

E-mail: n-kohei@sophia.ac.jp (K Noda)

Received 14 August 2006

Published 23 March 2007

Online at stacks.iop.org/JPhysCM/19/145279

Abstract

We have investigated orthorhombic $RMnO_3$ ($R = (Gd_{1-y}Tb_y)$) crystals near the phase boundary between the paraelectric A-type-antiferromagnetic (AF) phase (PA) and the ferroelectric transverse-spiral-AF one (FS). The spiral AF structure breaks inversion symmetry and induces the ferroelectric polarization through the inverse Dzyaloshinskii–Moriya (DM) interaction. We have found that the PA–FS phase boundary is located at $0.15 < y < 0.2$. In the $y = 0.15$ compound, PA and FS phases appear in the cooling scan, while FS is not observed in the warming scan. This result suggests that FS observed in $y = 0.15$ is a metastable state arising from the competition between PA and FS. Furthermore, we demonstrate the phase control between these competing phases by the application of the external magnetic field and external quasihydrostatic pressure.

(Some figures in this article are in colour only in the electronic version)

1. Introduction

Multiferroic materials are now the subject of renewed interest. Orthorhombic $RMnO_3$ ($R =$ rare earth ions) containing $TbMnO_3$ famous as the ‘magnetic control of the ferroelectric polarization’ [1] is one such multiferroic material, and some of them are simultaneously ferroelectric and antiferromagnetic. In $RMnO_3$, the magnetic frustration gives rise to the change of magnetic structures (canted A-type AF phase \Rightarrow transverse spiral AF one \Rightarrow E-type AF one) as a function of the ionic radius of R , and such magnetic frustration comes from the competition between the nearest neighbour (NN) ferromagnetic and the next NN antiferromagnetic (AF) interactions [2].

$TbMnO_3$ and $DyMnO_3$ show the transverse-spiral-AF phase, and in such a magnetic phase the spontaneous ferroelectric polarization is observed [3, 4]. Recently, it has been considered that such noncollinear-transverse-spiral magnetic structure breaks inversion symmetry and induces the ferroelectric polarization through the inverse Dzyaloshinskii–Moriya (DM)

interaction [3–7]. On the other hand, the canted-*A*-type-AF phase, which is observed in RMnO_3 with a larger ionic radius than $R = \text{Gd}$, does not induce the ferroelectric polarization, and anticorrelation between paraelectric canted-*A*-type-AF phase (PA) and ferroelectric transverse-spiral-AF phase (FS) is reported [8]. Therefore, the PA and FS phases compete with each other between GdMnO_3 and TbMnO_3 .

In this work, we have investigated the PA–FS phase boundary in RMnO_3 ($R = \text{Gd}_{1-y}\text{Tb}_y$) crystals in external magnetic field and under external quasihydrostatic pressure, to clarify the magnetoelectric properties of the phase boundary and to control the phase transition between PA and FS.

2. Experiments

All single crystals used in this work were prepared by the floating zone method (in Ar gas at a pressure of 0.25 MPa). We carried out an x-ray diffraction experiment to confirm that all crystals had an orthorhombic $Pbnm$ structure without any impurity phase. All specimens used in this study were cut along the crystallographic principal axes into a rectangular shape by means of an x-ray back-reflection Laue technique. Measurements of the temperature dependence of the dielectric constant and the spontaneous ferroelectric polarization in magnetic fields were carried out in a temperature-controllable cryostat equipped with a superconducting magnet that provides a field up to 8 T. The dielectric constant was determined with an *LCR* meter (Agilent, 4284 A). After the sample had been cooled under a poling electric field of 300–500 kV m⁻¹, the spontaneous electric polarization was obtained by the accumulation of a pyroelectric current while it was heated at a rate of 4 K min⁻¹. An external quasihydrostatic pressure was produced by a clamp-type piston cylinder cell using Fluorinert as the pressure-transmitting medium.

3. Results and discussion

3.1. Phase control through the chemical pressure

First, we investigated the PA–FS phase boundary by the control of the chemical composition of RMnO_3 ($R = (\text{Gd}_{1-y}\text{Tb}_y)$). As a result, we found that the phase boundary exists at $0.15 < y < 0.2$. Figures 1(a) and (b) show the temperature dependence of the dielectric constant along the *a* axis (ϵ_a) and the spontaneous ferroelectric polarization along the *a* axis (P_a) of RMnO_3 near the phase boundary ($y = 0.15$ and 0.20).

In the case of $y = 0.20$, only FS is observed below the paraelectric-AF–FS transition temperature in both cooling and warming scans. (See figures 1(a) and (b).) ϵ_a shows the divergent peak at 22 K, below which P_a appears. On the other hand, in the case of $y = 0.15$, the reentrant (paraelectric-AF \Rightarrow FS \Rightarrow PA) behaviour is observed. In the cooling scan, ϵ_a shows the divergent peak at 21 K and at this temperature P_a appears. However, P_a suddenly decreases below 16 K and finally disappears at 13 K. ϵ_a decreases with a decrease of P_a , and the value of ϵ_a in the ground state takes a small value compared with that of $y = 0.20$. This disappearance of P_a is originated from the magnetic phase transition from the transverse-spiral-AF phase to the canted-*A*-type AF one. This disappearance of P_a agrees well with the scenario of the anticorrelation between PA and FS [8]. In the warming scan, the FS is veiled by PA. (See figures 1(a) and (b).) Therefore, FS in the cooling scan is considered to be the metastable state. Such reentrant and hysteretic behaviour (or metastable state) is observed in $y = 0 - 0.15$, and the FS–PA transition temperature decreases with an increase of y . (See figure 1(c).) These results suggest that such reentrant behaviour arises from the competition between PA and FS.

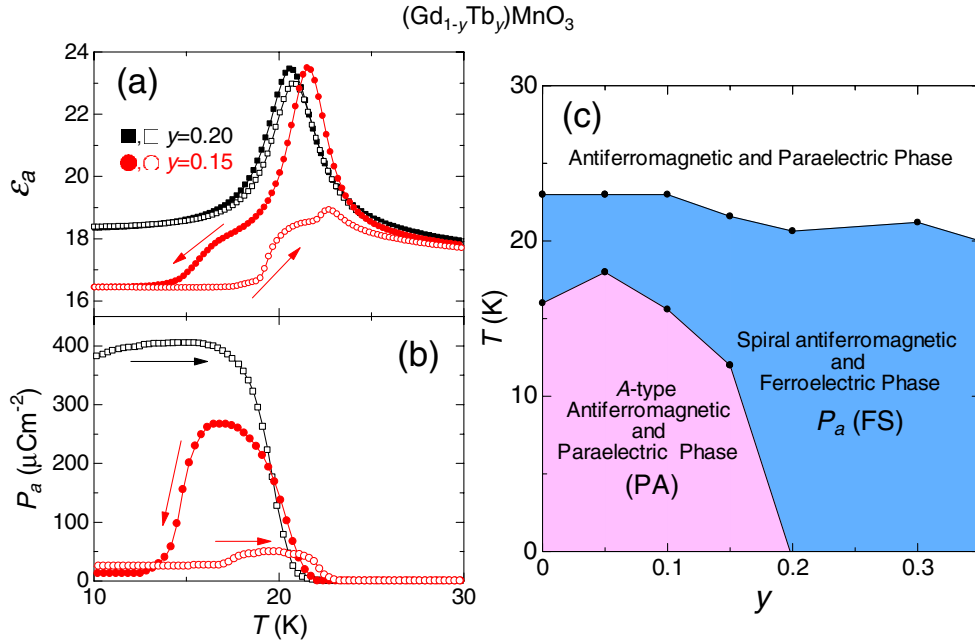


Figure 1. The temperature dependence of the dielectric constant along the a axis (ϵ_a) (a) and ferroelectric polarization along the a axis (P_a) (b) of $(\text{Gd}_{1-y}\text{Tb}_y)\text{MnO}_3$ ($y = 0.15$ and 0.20). Solid and open symbols display a cooling and warming scan respectively. Solid arrows indicate scan directions. (c) The magnetic and electric phase diagram of $(\text{Gd}_{1-y}\text{Tb}_y)\text{MnO}_3$ ($0 \leq y \leq 0.35$) obtained from a cooling scan without a magnetic field.

3.2. Phase control by the external magnetic field

Then, we demonstrate the phase control between PA and FS by the application of external magnetic field. The drastic phase conversion from FS to PA is realized by the application of the magnetic field parallel to the c axis (H_c) [8]. Therefore, in this work, we try to convert PA to FS by the application of the magnetic field. Figures 2(a) and (b) show the temperature dependence of ϵ_a and P_a in the magnetic field parallel to the b axis (H_b) in $y = 0.15$.

In $H_b \leq 4$ T the reentrant ferroelectric transition is observed, and at this transition temperature the dielectric anomaly appears, while such reentrant transition and dielectric anomaly do not occur in a zero magnetic field. (See figures 2(a) and (b).) The ferroelectric phase, which is observed in higher temperatures, is FS. On the other hand, the ferroelectric phase (FE), which appears by the application of H_b at a lower temperature, is considered to arise from the magnetic order of Gd $4f$ moments, and such a ferroelectric phase has already been reported in previous works [9–11]. (However, the magnetic structure of FE has not yet been clarified.) These ferroelectric phases are separated by PA, and this result suggests that these ferroelectric phases have no relation to each other.

Then, in $H_b \geq 5$ T, PA changes to the ferroelectric phase (FA) by the application of H_b . P_a emerges by the application of H_b and the value of ϵ_a becomes large gradually with the increase of H_b . (See the temperature region between 10 and 15 K in figures 2(a) and (b).) However, the decrease of P_a is observed at around the PA–FS transition temperature in $H_b \leq 4$ T. These results suggest that, in FA, the strong competition between PA and FS is induced by the application of H_b above 5 T, and such competition seems to cause the coexistence of PA

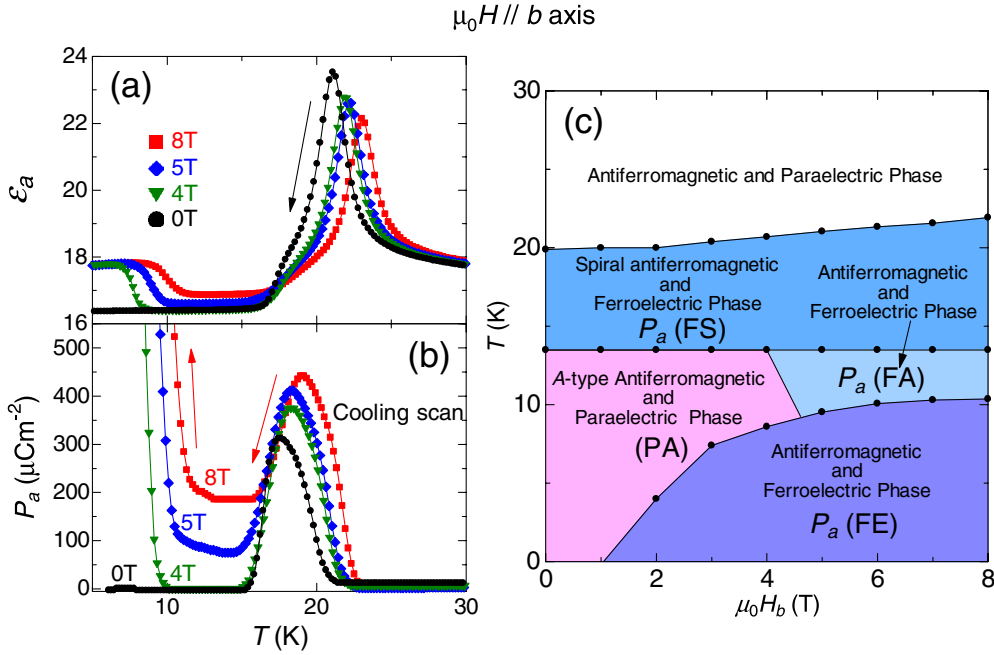


Figure 2. The temperature dependence of dielectric constant along the a axis (ϵ_a) (a) and ferroelectric polarization along the a axis (P_a) (b) of $(\text{Gd}_{1-y}\text{Tb}_y)\text{MnO}_3$ ($y = 0.15$) in the external magnetic field parallel to the b axis (H_b). Only the cooling scan data are displayed. (c) The magnetic and electric phase diagram of $(\text{Gd}_{1-y}\text{Tb}_y)\text{MnO}_3$ ($y = 0.15$) in H_b in a cooling scan.

and FS, while the anticorrelation between PA and FS is observed and such coexistence does not occur in H_c [8].

The electromagnetic phase diagram of $y = 0.15$ in H_b is shown in figure 2(c). FE appears above 2 T, and the ferroelectric transition temperature increases by the application of H_b below 10 K. FS is observed above 13 K. The ferroelectric transition temperature of FS increases by the application of H_b , while the transition temperature, at which the P_a disappears or decreases, is constant. Between these ferroelectric phases, FA is observed in H_b above 5 T. The influence of the $4f$ moments seems to exist below 10 K, because FE is observed below 10 K. Therefore, the ferroelectric phases observed above 10 K are considered to be originated from the magnetic structure of Mn $3d$ spins only. So, in FA, the coexistence of PA and FS is ascribed to the competition between the spiral AF and canted A -type AF phases of Mn $3d$ spins. These results suggest that FS is enhanced by the application of H_b , while PA is suppressed. This effect of H_b is the same as the effect of increase of y in figure 1(c).

3.3. Phase control by the external pressure

In this section, we discuss the effect of the external quasihydrostatic pressure (P_{ex}) on the magnetoelectric properties in orthorhombic RMnO_3 crystals. In LaMnO_3 , at room temperature, the linear decrease of the lattice parameters with an increase of P_{ex} is reported [12]. Therefore, the effect of P_{ex} on the magnetoelectric phases is considered to be the same as the effect of the increase of y in figure 1(c).

Figures 3(a) and (b) show the temperature dependence of ϵ_a and P_a under P_{ex} respectively. As shown in figures 3(a) and (b), PA easily collapses into FS with an increase of P_{ex} . The value

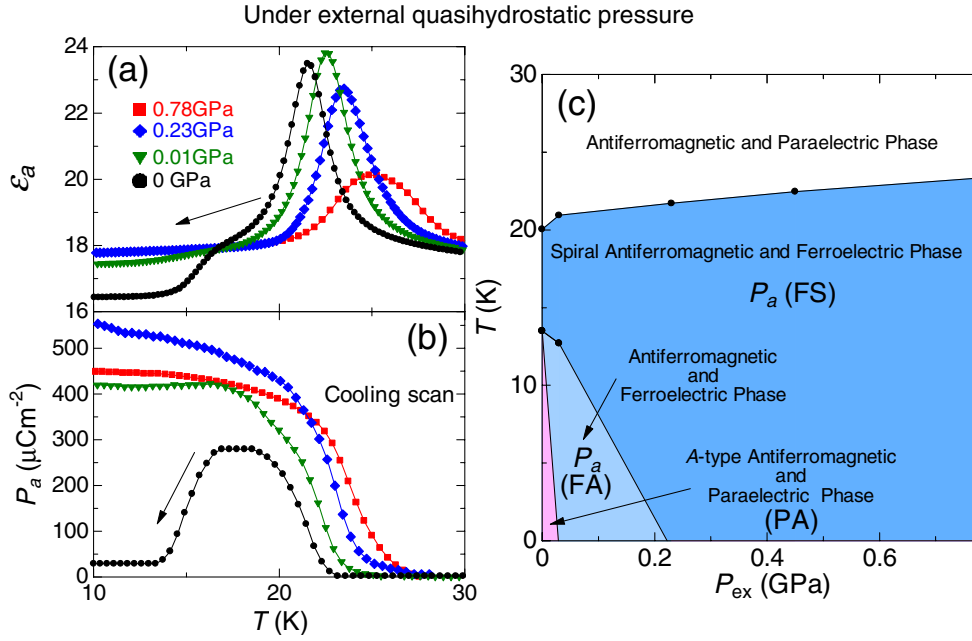


Figure 3. The temperature dependence of the dielectric constant along the a axis (ϵ_a) (a) and ferroelectric polarization along the a axis (P_a) (b) of $(\text{Gd}_{1-y}\text{Tb}_y)\text{MnO}_3$ ($y = 0.15$) in the external quasihydrostatic pressure (P_{ex}). Only the cooling scan data is displayed. (c) The magnetic and electric phase diagram of $(\text{Gd}_{1-y}\text{Tb}_y)\text{MnO}_3$ ($y = 0.15$) under P_{ex} in a cooling scan.

of ϵ_a in the ground state becomes large with an increase of P_{ex} . At 0.01 GPa, the value of ϵ_a is a little smaller than others, and a small decrease of P_a is observed. This result suggests that the coexistence of PA and FS occurs under 0.01 GPa. (The main phase is FS, but PA remains as a minor phase. Therefore, this phase is considered to be same as FA observed in H_b .)

The electromagnetic phase diagram under P_{ex} is shown in figure 3(c). As shown in figure 3(c), PA is drastically transected into FS by the application of P_{ex} . As expected, this result shows the same behaviour as the increase of y in figure 1(c). This result agrees well with the scenario of the anticorrelation between PA and FS [8], and indicates that the transverse-spiral-AF phase, which induces the ferroelectric polarization, arises from the magnetic frustration due to the increase of orthorhombic distortion.

4. Summary

In summary, we have studied the dielectric and magnetic properties of a $(\text{Gd}_{1-y}\text{Tb}_y)\text{MnO}_3$ single crystals. We have found the PA–FS phase boundary at around $0.15 < y < 0.2$ in a zero magnetic field. In addition, we have observed the reentrant (paraelectric phase \Rightarrow ferroelectric one \Rightarrow paraelectric one) phase transition in the cooling scan. Such reentrant behaviour probably arises from the strong competition between PA and FS. The phase control is achieved by the application of H_b and P_{ex} . In contrast to the case of the application of H_c [8], the coexistence between PA and FS is induced by the application of H_b . In such a coexisting phase, partial P_a is observed; however, the microscopic origin of this ferroelectric polarization has not yet been clarified. These results suggest that H_b enhances FS and suppresses PA in RMnO_3 . On the other hand, the drastic phase transition from PA to FS occurs by the application of

P_{ex} . Therefore, the magnetic frustration due to the increase of the orthorhombic distortion is considered to be the most important origin of the drastic phase transition, which provides an improved understanding of the mechanism of the magnetoelectric effect in multiferroic materials.

Acknowledgments

This work was supported by a Grant-in-Aid for Scientific Research (C) from the Japan Society for Promotion of Science, and by a Grant-in-Aid for Scientific Research on the Priority Area ‘High field spin science in 100 T’ (No 451) from the Ministry of Education, Culture, Sports, Science and Technology (MEXT).

References

- [1] Kimura T, Goto T, Shintani H, Ishizaka K, Arima T and Tokura Y 2003 *Nature* **426** 55
- [2] Kimura T, Ishihara S, Shintani H, Arima T, Takahashi K, Ishizaka K and Tokura Y 2003 *Phys. Rev. B* **68** 060403(R)
- [3] Kenzelmann M, Harris A, Jonas S, Broholm C, Schefer J, Kim S, Zhang C, Cheong S, Vajk O and Lynn J 2005 *Phys. Rev. Lett.* **95** 087206
- [4] Arima T, Goto T, Yamasaki Y, Miyasaka S, Ishii K, Tsubota M, Inami T, Murakami Y and Tokura Y 2005 *Phys. Rev. B* **72** 100102
- [5] Katsura H, Nagaosa N and Balatsky A 2005 *Phys. Rev. Lett.* **95** 057205
- [6] Mostovoy M 2006 *Phys. Rev. Lett.* **96** 067601
- [7] Sergienko I and Dagotto E 2006 *Phys. Rev. B* **95** 094434
- [8] Goto T, Yamasaki Y, Watanabe H, Kimura T and Tokura Y 2005 *Phys. Rev. B* **72** 220403(R)
- [9] Kuwahara H, Noda K, Nagayama J and Nakamura S 2005 *Physica B* **359–361** 1279
- [10] Noda K, Nagayama J, Nakamura S and Kuwahara H 2005 *J. Appl. Phys.* **97** 10C103
- [11] Noda K, Nakamura S and Kuwahara H 2005 *IEEE Trans. Magn.* **41** 2814
- [12] Loa I, Adler P, Grzechnik A, Syassen K, Schwarz U, Hanfland M, Rozenberg G, Gorodetsky P and Pasternak M 2001 *Phys. Rev. Lett.* **82** 125501